

Degradation Mode Survey Candidate Titanium - Base Alloys for Yucca Mountain Project Waste Package Materials

G.E. Gdowski

December 1997



This is an informal report intended primarily for internal or limited external distribution. The opinions and conclusions stated are those of the author and may or may not be those of the Laboratory.

Work performed under the auspices of the U.S. Department of Energy by the Lawrence Livermore National Laboratory under Contract W-7405-ENG-48.

DISCLAIMER

This document was prepared as an account of work sponsored by an agency of the United States Government. Neither the United States Government nor the University of California nor any of their employees, makes any warranty, express or implied, or assumes any legal liability or responsibility for the accuracy, completeness, or usefulness of any information, apparatus, product, or process disclosed, or represents that its use would not infringe privately owned rights. Reference herein to any specific commercial product, process, or service by trade name, trademark, manufacturer, or otherwise, does not necessarily constitute or imply its endorsement, recommendation, or favoring by the United States Government or the University of California. The views and opinions of authors expressed herein do not necessarily state or reflect those of the United States Government or the University of California, and shall not be used for advertising or product endorsement purposes.

This report has been reproduced
directly from the best available copy.

Available to DOE and DOE contractors from the
Office of Scientific and Technical Information
P.O. Box 62, Oak Ridge, TN 37831
Prices available from (615) 576-8401, FTS 626-8401

Available to the public from the
National Technical Information Service
U.S. Department of Commerce
5285 Port Royal Rd.,
Springfield, VA 22161

Degradation Mode Survey
Candidate Titanium - Base Alloys for
Yucca Mountain Project Waste Package Material

G.E. Gdowski
Lawrence Livermore National Laboratory
Livermore, California 94550

Table of Contents

	Page
Table of Contents	i
1.0 Introduction	1
2.0 Physical Metallurgy and Microstructure	4
2.1 Introduction	4
2.2 Phase Diagrams	4
2.3 Bulk Microstructure	5
3.0 Tensile and Physical Properties	7
4.0 Weldability and Weldment Corrosion	10
5.0 Corrosive Environment Considerations	11
6.0 Oxide Film	12
6.1 Film Composition and Structure	12
6.2 Pourbaix Diagram	14
7.0 General Corrosion Resistance	15
8.0 Pitting Corrosion	17
9.0 Crevice Corrosion	18
9.1 Temperature	19
9.2 Solution Chemistry and pH	20
9.4 Physical Characteristics of a Susceptible Crevice	22
9.5 Alloy Composition	23
9.6 Surface Condition	25
9.7 Metal Potential	26
10.0 Sustained Load Cracking	26
11.0 Hydrogen Embrittlement	28
11.1 Mechanism	29
11.2 Physical Properties	29
11.3 Effect of the Surface Layer on Hydrogen Uptake	31
11.4 Effect of pH on Hydrogen Uptake	31
11.5 Galvanic Coupling	32
12.0 Stress Corrosion Cracking	33
13.0 Galvanic Corrosion	35
14.0 Radiation Environment	38
15.0 Additional Corrosion Studies of Titanium Alloys	39
16.0 Conclusions	41
17.0 Acknowledgments	42
18.0 References	43
19.0 Appendix A	49
20.0 Appendix B	53

1.0. Introduction

The Yucca Mountain Site Characterization Project (YMP) is evaluating materials from which to fabricate high-level nuclear waste containers (hereafter called waste packages) for the potential repository at Yucca Mountain, Nevada [MCC96]. Because of their very good corrosion resistance in aqueous environments titanium alloys are considered for container materials [MCC96]. Consideration of titanium alloys is understandable since about one-third (in 1978) of all titanium produced is used in applications where corrosion resistance is of primary importance [MIN78]. Consequently, there is considerable amount of data which demonstrates that titanium alloys, in general, but particularly the commercial purity and dilute α grades, are highly corrosion resistant [SCH86, FEI70, COV77].

The highest resistance to corrosion and hydrogen embrittlement effects is found in commercial purity (C.P.), dilute α -grades of Ti (titanium content ≥ 98.9 wt.%), and other titanium alloys with Pd additions. Titanium alloys commonly used in corrosion resistant equipment or proposed for this purpose are shown in Table 1.1. These alloys are different grades of C.P. titanium (Ti Gr 1-4), α -Ti with small Pd content (Ti Gr 7, 11, 16 and 17), the Ti-0.3%Mo-0.8%Ni alloy (Ti Gr 12), and other higher alloyed Ti alloys with Pd additions. (Note: Ti Gr 11 and 17 have the same Pd content as Ti Gr 7 and 16, respectively, but they have a lower impurity content and hence a higher cost. Ti Gr 7 is more commonly used than Ti Gr 11.)

Both the titanium-palladium alloys and the Ti Gr 12 alloy are used in applications requiring better corrosion resistance than that of the C.P. titanium. Titanium-palladium alloys are used where the corrosive media is mildly reducing or fluctuates between oxidizing and reducing. The lower Pd addition alloys (Ti Gr 16 and 17) are not as corrosion resistant as the high Pd addition alloy (Ti Gr 7 and 11), however, Ti Gr 16 and 17 have significantly better corrosion resistance than C.P. titanium and is less costly than Ti Gr 7 [SCH93]. It should be noted that Ti Gr 16 is a new alloy and, therefore, limited amounts of information are available. Palladium additions are within the solid solution solubility limits in α -Ti. The characteristics of good fabricability, weldability, and strength level are similar to those of corresponding unalloyed titanium grades [LAM90]. Ti Gr 12 has better corrosion resistance and higher strength than those of C.P. titanium. However, the corrosion resistance is generally not as good as Ti Gr 7.

This report will discuss the corrosion characteristics of Ti Gr 2, 7, 12, and 16. The more highly alloyed titanium alloys which were developed by adding a small Pd content to higher strength Ti alloys in order to give them better corrosion resistance will not be considered in this report. These alloys are all two phase (α and β) alloys. The palladium addition while making these alloys more corrosion resistant does not give them the corrosion resistance of the single phase α and near- α (Ti Gr 12) alloys.

Table 1.1. Compositions of higher corrosion resistant titanium alloys. The alloys considered corrosion resistant are the commercial purity alloys, the palladium containing alloys, and Ti Grade 12. Compositions from reference ASTM B 265.

ASTM Designation	C (max)	Fe (max)	H (max)	N (max)	O (max)	Ti	Pd	Ni	Mo	Al	V	Co	Residuals, max each	Residuals, max total
Grade 1	0.08	0.20	0.015	0.03	0.18	bal							0.1	0.4
Grade 2	0.08	0.30	0.015	0.03	0.25	bal							0.1	0.4
Grade 3	0.08	0.30	0.015	0.05	0.35	bal							0.1	0.4
Grade 4	0.08	0.50	0.015	0.05	0.40	bal							0.1	0.4
Grade 7	0.08	0.30	0.015	0.03	0.25	bal	0.12 - 0.25						0.1	0.4
Grade 11	0.08	0.20	0.015	0.03	0.18	bal	0.12 - 0.25						0.1	0.4
Grade 12	0.08	0.30	0.015	0.03	0.25	bal		0.6 - 0.9	0.2 - 0.4				0.1	0.4
Grade 16	0.08	0.30	0.015	0.03	0.30	bal	0.04 - 0.08						0.1	0.4
Grade 17	0.08	0.20	0.015	0.03	0.18	bal	0.04 - 0.08						0.1	0.4
Grade 18	0.08	0.25	0.015	0.03	0.15	bal	0.04 - 0.08			2.5 - 3.5	2.0 - 3.0		0.1	0.4
Grade 20	0.05	0.30	0.02	0.03	0.12	bal	0.04 - 0.08			3.0 - 4.0	7.5 - 8.5		0.1	0.4
Grade 24	0.08	0.40	0.015	0.05	0.20	bal	0.04 - 0.08			5.5 - 6.75	3.5 - 4.5		0.1	0.4
Grade 25	0.08	0.40	0.0125	0.05	0.20	bal	0.04 - 0.08	0.3 - 0.8		5.5 - 6.75	3.5 - 4.5		0.1	0.4
Grade 30	0.08	0.30	0.015	0.03	0.25	bal	0.04 - 0.08					0.20 - 0.80	0.1	0.4
Grade 31	0.08	0.30	0.015	0.05	0.35	bal	0.04 - 0.08					0.20 - 0.80	0.1	0.4

2.0 Physical Metallurgy and Microstructure

2.1 Introduction

Pure titanium is an allotropic element; that is, it has more than one crystallographic form. Above 883°C it has a body-centered cubic (bcc) crystal structure, which is called the beta (β) phase. Below 883°C, it transforms to a hexagonal closed-packed (hcp) structure, which is called the alpha (α) phase.

Alloying elements can either stabilize the β or α phase microstructure. Some α -phase stabilizers, which increase the temperature to which the α phase is stable, are Al, Ga, Ge, Sn, C, O, and N. Some β -phase stabilizers, which stabilize the β -phase to lower temperatures, are Fe, Mn, Cr, Mo, and V. Substitutional elements generally tend to be β -phase stabilizing. The β -transus temperature is the lowest equilibrium temperature at which the α or $\alpha + \beta$ structure transforms to all β microstructure.

Two groups of elements stabilize the β phase structure. The group of elements that are miscible in the β phase, including Mo, V, Ta, and Nb, are called the β isomorphous group. Elements in the other group promote the eutectoid reaction at temperatures as much as 333°C below the β -transus temperature of unalloyed titanium. The eutectoid forming elements include Mn, Fe, Cr, Co, Ni, Cu, and Si.

2.2 Phase Diagrams

Three titanium alloys systems are considered: 1) commercially pure titanium (Ti Gr 2), 2) titanium with less than or equal to 0.2% Pd (Ti Gr 7 and 16), and 3) a dilute titanium alloy (Ti Gr 12). All three systems are α or near- α Ti alloys.

Ti Gr 7 and 16 are titanium alloys with a very small additions of palladium, 0.2 and 0.05 wt.% respectively. The phase diagram for the binary system Pd-Ti is shown in Fig. 2.1 [MAS90]. The maximum solubility of Pd in α titanium is about 2 wt.% at 595°C. As the temperature decreases from 595°C the solubility decreases. At 400°C the Pd solubility in α titanium is about 1 wt.%. At higher Pd concentrations there is a two-phase region of α -Ti(Pd) and an intermetallic phase. The intermetallic phase is either Ti_4Pd or Ti_2Pd ; the existence of the latter phase is uncertain.

The nominal Pd concentrations of Ti Gr 7 and 16 are both well below the solubility limit at 400°C. The higher Pd content alloy (Ti Gr 7) was developed such that all the Pd remains in solid solution.

Ti Gr 12 has small additions of Mo (0.3 wt.%) and Ni (0.8 wt.%). Nickel solubility in α titanium is small; less than 0.05 wt.% at 300°C. At temperatures below 765°C and nickel concentrations greater than 0.1 wt.%, an intermetallic phase Ti_2Ni forms (Fig. 2.2) [MAS90]. The solubility of molybdenum in α titanium is very small (below 0.1wt.%) at temperatures below 400°C. At higher molybdenum, concentrations there is a mixture of α -Ti and β (Mo,Ti) (Fig. 2.3) [MAS90]. The Ti Gr 12 microstructure is a mixture of α -Ti, Ti_2Ni intermetallic, and β -Ti.

2.3 Bulk Microstructure

The bulk microstructure of α -Ti alloys is dependent on heat treatment and working of the material [BOY85]. The α alloys (Ti Gr 2, 7, and 16) consist of equiaxed α grains after annealing cold-worked alloys above the recrystallization temperature range. The microstructure is hexagonal closed packed (hcp) below 890°C and body centered cubic (bcc) above about 913°C. The transition temperature is influenced by amounts and kinds of impurity elements present. Elongated α grains result from unidirectional working of the metal and are commonly found in longitudinal sections of rolled or extruded alloys.

Generally, two types of α , primary α and secondary α or transformed β , are present in titanium alloys [BOY85]. Primary α is that α which persists through heat treatment and cold working. Secondary α is that α produced by transformation of β with cooling. This can result from cooling from above the β transus or aging of nonequilibrium β . The α in these areas has a unique appearance and may be acicular or lamellar, platelike, serrated, or Widmanstätten [BOY85].

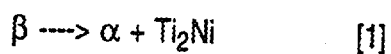
The microstructure of titanium alloys is influenced by heat treatment and processing history [BOY85]. With increasing cooling rate, the spacing of the lamellar α (or martensite, depending on the alloy and cooling rate) becomes finer. With increasing forging or heat-treatment temperature, the amount of transformed β increases until the forging or heat-treatment temperature is above the β transus, at which point the structure is 100% transformed β . Sufficient working of the cast Widmanstätten structure at a temperature below the β transus causes recrystallization of the lamellar structure to a more equiaxed structure. Sufficient working and proper heat treatment can produce a completely equiaxed crystal structure.

Acicular or lamellar α is the most common transformation product formed from β during cooling [BOY85]. It results from nucleation and growth occurring on specific crystallographic planes of the prior β matrix. Precipitation normally occurs on multiple variants or orientations of this family of habit planes. A "colony" is a packet or cluster of acicular α grains aligned in the same orientation. When correlating this type of microstructure with properties such as fatigue or fracture toughness, colony size is an important microstructural feature. The multiple orientations of α have a basket weave appearance characteristic of a Widmanstatten structure. A singular orientation results from lamellar α forming from small β grains.

Other α microstructures can occur, depending on nucleation conditions [BOY85]. Long grains of α that are produced along preferred planes in the β matrix take on a platelike appearance. Grains of irregular size and with jagged boundaries, called "serrated α " are also possible.

The microstructures of Ti Gr 7 and 16 are the same as for equivalent grades of unalloyed titanium, since only small amounts of α soluble palladium are added to make these Ti-Pd alloys. Titanium-palladium intermetallic compounds capable of being formed in this system have not been reported to occur in Ti Gr 7 and 16 with normal heat treatments. Transformation temperatures for these alloys are expected to be similar to those of unalloyed titanium.

The microstructure of Ti Gr 12 consists of equiaxed α grains with 10 -15% (by volume) of β phase located primarily along grain boundaries and at grain boundary triple points. The intermetallic compound Ti_2Ni is observed at α / β interfaces and within the β phase. The Ti_2Ni phase forms through the eutectoid reaction



Acicular α microstructures are found primarily in welds or heat affected zone [MOL83].

Unless heat treatments are performed in an inert atmosphere, oxygen and nitrogen will react with titanium and form a hard brittle layer referred to as an " α case" [BOY85]. (Oxygen and nitrogen are both α stabilizers.) This " α case" must be removed before the part is put into service.

3.0 Tensile and Physical Properties

The tensile requirements of some commercially available titanium alloys at room temperature and 300°C are shown in Table 3.1. There are significant increases in yield strength and ultimate tensile strength as the impurity content, particularly that of oxygen and iron, increases. Similarly, intentional alloying additions produce significant strength increases. The small alloying additions in Ti Gr 12 result in a significant strengthening of the titanium by introducing a small amount of β phase to the microstructure, and by solid solution strengthening. However, the small Pd additions in Ti Gr 7 and 16 do not significantly change the mechanical properties in comparison to Ti Gr 2, an alloy with a similar amount of impurities.

One disadvantage of titanium and its alloys is that their strength decreases rather rapidly with increasing temperature (Fig. 3.1). This is due to the strong temperature dependence of interstitial solute strengthening mechanisms. The yield and ultimate tensile strength values for Ti Gr 12 always remain higher relative to unalloyed Ti Gr 2 and Ti-Pd (Ti Gr 7).

Table 3.1. Tensile requirements for corrosion resistant titanium alloys. Data taken from ASTM B 265.

ASTM Designation	Tensile Strength		Yield Strength, 0.2% offset				Elongation in 50 mm	Bend Test	
	<u>minimum</u>		<u>minimum</u>		<u>maximum</u>			min. %	Under 1.8 mm in thickness
	ksi	MPa	ksi	MPa	ksi	MPa			
Grade 1	35	240	25	170	45	310	24	3 T	4 T
Grade 2	50	345	40	275	65	450	20	4 T	5 T
Grade 3	65	450	55	380	80	550	18	4 T	5 T
Grade 4	80	550	70	483	95	655	15	5 T	6 T
Grade 7	50	345	40	275	65	450	20	4 T	5 T
Grade 11	35	240	25	170	45	310	24	3 T	4 T
Grade 12	70	483	50	345	—	—	18	4 T	5 T
Grade 16	50	345	40	275	65	450	20	4 T	4 T
Grade 17	35	240	25	170	45	310	24	3 T	4 T
Grade 18	90	620	70	483	—	—	15	5 T	6 T
Grade 20	115	793	110	759	—	—	15	6 T	6 T
Grade 24	130	895	120	828	—	—	10		
Grade 25	130	895	120	828	—	—	10		
Grade 30	50	345	40	275	—	—	20	4 T	5 T
Grade 31	65	450	55	380	—	—	18	4 T	5 T

Allowable stress values from the ASME pressure vessel code for titanium alloys also decrease as a function of increasing temperature (Table 3.2) [COV89]. The allowable stress for Ti Gr 12 are higher at all temperatures than are those for Ti Gr 2 (unalloyed Ti) and Ti Gr 7 (Ti-0.2%Pd). At 260°C (500°F), the design stress for Ti Gr 12 is 70% greater than that of either Ti Gr 2 or 7.

Table 3.2. Design stresses (ksi) for titanium plate^{a,b} [COV89].

UNSR5-2400

For metal temperatures not exceeding (°C)	Gr 2 (Ti-50A)	Gr 3	Gr 7 (Ti-0.2Pd)	Gr 12 (Ti-0.3Mo-0.8Ni)
38	125	16.3	125	17.5
93	10.9		10.9	16.4
149	9.0	11.7	9.0	14.2
204	7.7		7.7	12.5
260	6.6		6.6	11.4
316	5.7	6.0	5.7	

a - ASME Section VIII, Division 1 - Pressure Vessels

b - Design stresses for Ti Gr 16 should be similar to Ti Gr 2 and 7, since this property is a function of impurity content.

The physical properties of titanium and its alloys must be considered when designing or fabricating equipment from these materials (Table 3.3) [SCH86]. Titanium alloys have densities slightly over half those of iron or copper-based alloys. The modulus of elasticity of titanium is also about half that of steel. Specific heat and thermal conductivity are similar to those of stainless steel. Titanium has a relatively high electrical resistivity and low thermal expansion coefficient.

Table 3.3. Physical properties of some titanium alloys [SCH86].

Property	Titanium Alloy			
	Gr 1	Gr 2	Gr 3	Gr 12
Density (g/cm ³)	4.54	4.54	4.54	4.55
Melting point (°C)	1660	1678	1660	—
Beta transus (°C)	883	913	921	885
Specific heat (joules/g/°C)	0.51	0.52	0.52	0.54
Thermal Conductivity (W/m °K)	15.6	16.4	16.4	19.0
Coefficient of expansion (10 ⁻⁶ /°C)	9.0	9.0	9.0	9.0
Electrical resistivity (μohm·cm)	56	56	57	52
Modulus of elasticity (10 ³ MPa)	103	103	103	103
Poisson ratio	0.34	0.34	0.34	0.34

Note: Ti Gr 7 and 16 should have similar properties to Ti Gr 2, since these properties are primarily dependent on impurity content. The exception may be electrical resistivity.

4.0 Weldability and Weldment Corrosion

Titanium alloys are readily weldable with processes that exclude interstitial contaminants such as C, O₂, H₂, and N₂ from the fusion and heat-affected zones of the weldment. These processes include gas-tungsten-arc welding (GTAW), gas-metal-arc welding (GMAW), resistance, plasma, inertia (friction), pressure, and electron beam welding methods [SCH86].

The use of inert-gas shielding during welding is essential due to the high affinity of titanium for oxygen, nitrogen, carbon, and hydrogen. These elements dissolve interstitially and can result in severe embrittlement when present in relatively small quantities. Therefore, additional inert gas shielding must be provided during welding to protect those parts close to the molten pool. Good techniques for inert gas shielding of welds, which involve use of trailing shields as well as shielding of the root surfaces of the weldment, have been developed. Use of these techniques, together with careful procedures to exclude all moisture, dirt and other foreign matter from the weld area, assure good welds [COV89].

Proper attention to the details described above results in weld properties equivalent to those of the base metal. Contamination of welds results in loss of ductility and toughness, as well as degraded corrosion resistance.

Weldments of Ti Gr 1-4, Gr 7, and Gr 12 generally exhibit corrosion resistance similar to that of their unwelded, wrought counterparts. Therefore, titanium alloy weldments and associated heat-affected zones generally do not experience corrosion limitations in welded components when normal passive conditions prevail for the base metal. However, under marginal or active conditions (for corrosion rates ≥ 0.10 mm/yr or 4 mils/yr) weldments may experience accelerated corrosion attack relative to the base metal, depending on alloy composition. The increasing impurity (iron, sulfur, oxygen) content associated with the coarse, transformed- β microstructure of weldments appears to be a factor.

5.0 Corrosive Environment Considerations

This section is concerned with the aqueous phase corrosion of the titanium alloys. This includes corrosion that can occur in bulk aqueous phases and also corrosion that occurs in thin water films present on surfaces under high relative humidities. The potential repository at Yucca Mountain is in the unsaturated zone, that is, it is located above the water table, and therefore, the maximum expected water vapor pressure is ambient pressure. For clean surfaces significant water film formation is limited to temperatures at or below the ambient boiling point of unconstrained water. Crevices and hygroscopic salts will raise the temperatures at which water film formation on the waste package is possible.

The liquid water that does come in contact with the waste containers is expected to have a low ionic content (sulfate, chloride, carbonate), a near neutral to moderately elevated pH, and to be oxidizing. However, bounding aqueous solution compositions are also considered for credible water contact scenarios. These are: concentrated solutions, because of evaporation or boiling; low pH solutions because of microbial activity; and high pH solutions because of cementitious material in the repository.

Various thermal loading scenarios have been considered for the repository with maximum container temperatures not expected to exceed 250-300°C. Since the repository site will be at atmospheric pressure aqueous corrosion phenomena will be limited to temperatures which are determined by the hygroscopic salts present. For instance, saturated NaCl solutions have a

boiling point of about 109°C, and CaCl_2 solutions can have boiling points of up to at least 150°C. The possibility of galvanic coupling of the titanium alloys to other materials is also considered because of the potential use of multiple metallic barriers.

6.0 Oxide Film

6.1 Film Composition and Structure

The excellent corrosion resistance of titanium alloys results from the formation of a very stable, continuous, highly adherent, and protective oxide film. Because titanium metal itself is highly reactive and has an extremely high affinity for oxygen, these beneficial surface oxide films form spontaneously and instantly when fresh metal is exposed to air and/or moisture. In fact, a damaged oxide film can generally heal itself instantaneously if at least a few parts per million of oxygen or water (moisture) are present in the environment. However, anhydrous conditions in the absence of a source of oxygen may result in titanium corrosion, because the protective film may not be regenerated if damaged.

The nature, composition, and thickness of the protective surface oxides that form on titanium alloys depends on environmental conditions, and this in turn significantly affects the material's corrosion resistance. According to Tomashov et al. [TOM82] film composition varies from TiO_2 at the surface, through Ti_2O_3 below the surface, to TiO at the metal interface. High temperature oxidation tends to promote the formation of the chemically-resistant, highly-crystalline form of TiO_2 , known as "rutile". Lower temperature oxidation often result in formation of the anatase form of TiO_2 , or a mixture of rutile and anatase. Although these naturally-formed films are typically less than 10 nm [AND64] thick and are invisible to the naked eye, they are extremely resistant to degradation. However strongly oxidizing solutions, such as immersion in concentrated HNO_3 , will accelerate their growth.

Oxides formed on Ti alloys in aqueous environments at elevated temperatures (95°C) are amorphous [MAT84]. The oxide consists of an outer layer of TiO_2 and a few atomic layers of suboxide (Ti_2O_3) next to the oxide/metal interface. The structure of the oxide was not significantly influenced by the oxygen content (saturated or deoxygenated) or NaCl content (0 or 1 wt.%). In neutral water, the outer oxide layer was anhydrous, that is, TiO_2 . This was thought to be significant since hydrated titanium oxide is slightly soluble in acid solutions, whereas anhydrous oxide is not. It was concluded that the anhydrous oxide is more corrosion-resistant.

In water-saturated bentonite at 95°C, the constituents of montmorillonite (the main component of bentonite) are embedded within the oxide layer. X-ray photoelectron spectroscopy analysis indicates that the simple oxides of the constituent species (Si^{4+} , Al^{3+} , and Mg^{2+}) are present in the oxide. These species appear to be primarily in the outer layers of the oxide and their concentrations decrease as the metal oxide layer is approached. No difference between the oxide structure formed on Ti and Ti-0.2%Pd could be detected.

In contrast to their behavior in neutral aqueous solutions, the oxide layer composition is affected by minor alloying elements when the material is immersed in acid solutions. For Ti-0.2%Pd, there is an enrichment of the more noble Pd metal in the oxide layer caused by dissolution of titanium atoms. The effect of the enrichment in Pd is to increase the ability of the alloy to repassivate. A similar effect has been suggested for titanium alloyed with small amounts of nickel. However the role nickel in enhancing the corrosion resistance of Ti-0.8%Ni-0.3%Mo (Ti Gr 12) is the subject of some debate.

It is agreed that nickel is involved in passivation of the alloy, and that the nickel is somehow present in the passive film. Two mechanisms have been proposed. In dilute Ti-Ni alloys, where nickel is present as Ti_2Ni , one mechanism is that the cathodic hydrogen evolution reaction proceeds on Ti_2Ni particles at the surface [TOM82]. This cathodic reaction causes passivation by enhancing the passivating anodic current. The other mechanism suggests that nickel dissolves from the Ti_2Ni particles and is subsequently redeposited as metallic nickel on the titanium surface [SED72]. It is suggested that Ni atoms are then stabilized in the passive film due to a strongly-bound surface complex involving coordination of the Ni atoms by surrounding titanium oxide species. X-ray photoelectron spectroscopy of surfaces of dilute Ti-Ni alloys, after corrosion in acid sulfate solutions, indicate that the oxide film is enriched in nickel, which is in the zero oxidation state [PET80]. It has also been suggested that the passivation of Ti Gr 12 during crevice corrosion is not simply due to enhancement of the hydrogen reduction reaction, but rather that nucleation and growth of a protective surface layer that incorporates nickel as Ni atoms [MCK84].

6.2 Pourbaix Diagram

The Pourbaix (potential-pH) diagram is useful in understanding the corrosion behavior of titanium by recognizing the conditions under which the oxide film is thermodynamically stable. Lee [LEE81]

has constructed potential - pH diagrams for titanium in water at temperatures from 25 to 300°C. The Pourbaix diagrams for the Ti-H₂O system at 25, 150, and 300°C are shown in Fig. 6.1. These diagrams show the wide regime over which the passive TiO₂ film is predicted to be stable, based on thermodynamic considerations. Oxide stability over the full pH scale is indicated over a wide range of highly oxidizing to mildly reducing potentials, whereas oxide film breakdown and the resultant corrosion of titanium occurs under reducing acidic conditions. At temperatures higher than 150°C, strong alkaline (> pH 15) solutions tend to dissolve TiO₂, forming the acid oxy-anion of titanium (HTiO₃⁻). The stable domain of HTiO₃⁻ is expanded as the temperature increases. Thus, a region of dissolution of titanium in alkaline solutions is expected at higher temperatures. The standard electrode potential for the Ti-Ti⁺⁺ reaction is -1.628 V at 25°C and becomes more negative with increasing temperature to a value of -1.665 at 300°C. It was observed that the stability of titanium and its oxides in acidic solution increases with increasing temperature, but their stability is decreased in alkaline solutions at higher temperatures. According to the Pourbaix diagram, neutral or slightly alkaline water at higher temperatures should not affect the TiO₂ film.

7.0 General Corrosion Resistance

In 1978 it was estimated that about one-third of all titanium produced is used in applications where corrosion resistance is of primary importance [MIN78]. Consequently there are data which demonstrate that titanium alloys, in general, but particularly the commercial purity and dilute α Ti grades, are highly corrosion resistant [FEI70, COV77].

Titanium retains its corrosion resistance to 315°C or more. At higher temperatures, the film is destroyed because oxygen diffuses into the base metal, greatly lowering corrosion resistance. Although the TiO₂ film is highly corrosion resistant, it will be attacked by a few substances, including hot concentrated HCl, H₂SO₄, NaOH, and HF.

General corrosion rates that have been reported in near-neutral aqueous solutions indicate that very low corrosion rates would be expected after the initial formation of the protective oxide film. At 95°C, the oxide layer was 60Å after 10 days, however, based on tests of 6 month duration, the long-term growth is expected to follow a logarithmic law, which as given by:

$$y = 8.7 + 3.65 \ln (t)$$

where t is time in seconds, and y is the oxide thickness in Å. Oxygen (saturated and deoxygenated) and NaCl (0 or 1%) concentration did not significantly affect the growth rate.

In water-saturated bentonite at 80°C the film growth rate was logarithmic and given by:

$$y = 5.5 \ln (t).$$

The relationship was based on exposures from 4 months to 2 years. However, longer exposure periods (years) indicate that the rate increases with time; this increase is thought to be due to the crystallization of the initially amorphous oxide layer, which allows easier ionic transport along grain boundaries [MAT90]. There was no significant difference in the corrosion rates for Ti and Ti-0.2%Pd.

The environment in which the oxide layer is formed significantly affects its corrosion resistance [BRA80]. Oxide layers formed in different environments at 25°C were subsequently immersed in 6N H₂SO₄. The potential of the specimens was monitored as a function of time. For all specimens, the potential decreased and eventually reached a stable value at about -0.65 V(SCE). This was thought to be due to a reduction of the oxide layer. Those specimens with oxide layers formed with both oxygen and water present showed the most resistance to reduction processes. Oxide layers formed in dry air had a factor of 3 or 4 less resistance.

A more corrosion-resistant oxide layer was found to be formed by thermal oxidation than by either anodization or pickling [SCH81]. Better corrosion resistance was found for thermally oxidized (677°C, 1 minute) specimens in solutions of less than 0.8 % HCl for 100 hr exposures. For 300 hr exposures thermal oxide stability is seen only for solution up to 0.5% HCl. Thermal oxide films are also very tenacious in simple acid pickling solutions, whereas anodized films can rapidly be removed by the acid pickle. In general, thermal oxide films must be sandblasted or processed in a caustic descaling bath to effect removal.

An enhanced short term benefit for thermal oxidation of Ti Gr 7 and 12 was also found for resistance to corrosion in the 0.8 HCl solutions [SCH81]. The benefit did not extend to longer times (100 hr exposures). However, the corrosion resistance of Ti Gr 7 and 12 was still better than that of Ti Gr 2 with or without the thermal oxide.

The thermal oxide layer on pure titanium enhanced its resistance to crevice corrosion and hydrogen embrittlement [SCH81]. Thermal oxidation can offer significant improvement in crevice

proceed autocatalytically within the crevice. Studies have determined that pH values as low as 0 to 1 may develop within active crevices [GRI68, MCK84]. The hydrogen produced as a cathodic by-product either recombines to form hydrogen gas molecules, which evolve from crevices, or is absorbed by interior crevice surfaces forming hydride layers.

Initiation and propagation of titanium alloy crevice corrosion is significantly influenced by temperature, solution chemistry / pH, the physical nature of the crevice, titanium alloy composition, metal surface condition, and metal potential. The following sections discuss the effects of each of these factors.

9.1 Temperature

Titanium susceptibility to crevice corrosion generally increases with increasing temperature [GRI68] provided other conditions are favorable for it to occur. Figure 9.1 shows susceptibility of three titanium alloys to crevice corrosion with increasing temperature and decreasing pH in a saturated NaCl solutions [SCH85]. Unalloyed titanium (Ti Gr 2) becomes susceptible at temperatures greater than 70°C at low to moderate pH values. At temperatures greater than 80-85°C it is susceptible to crevice corrosion in near neutral solutions. Ti Gr 12 becomes susceptible above 75°C, however relatively low pH's are required for crevice corrosion initiation. For temperatures below 100°C, pH levels must be below 2.5 in order for crevice corrosion to occur. Ti Gr 7 is the least susceptible to crevice corrosion. The minimum temperature for crevice corrosion susceptibility is similar to Ti Gr 12, however, much lower pH level are necessary to cause crevice corrosion. For temperature below 100°C, pH levels must be less than 1 for crevice corrosion to occur on Ti Gr 7.

9.2 Solution Chemistry / pH

Titanium is known to be susceptible to crevice corrosion in chloride, bromide, iodide, fluoride, and sulfate solutions. All other conditions considered equal, the threshold for crevice corrosion in fluoride-rich solutions occurs at lower temperatures and higher pH than for the chloride, bromide, iodide, and sulfate solutions [SCH92a]. Crevice corrosion threshold levels of chloride concentration are between 100 and 1,000 ppm, depending on temperature, pH, and the cathodic depolarizers present. Pure sulfate solutions tend to be more benign, with crevice attack occurring at higher sulfate concentrations (>1%) and temperatures (>82°C) [SCH87]. In general, crevice attack increases with increasing halide concentration, although some studies indicate a decreased susceptibility in the 1 to 2 M halide range.

Non-oxidizing cations that hydrolyze to form HCl at high concentrations and temperatures may aggravate localized attack. Salts of cations such as Mg^{+2} , Ca^{+2} , Zn^{+2} , and Al^{+3} may aggravate crevice corrosion, while salts of cations such as Na^+ , K^+ , and NH_4^+ will not [SMA81]. In addition, these hydrolyzable salt solutions can produce a special form of localized corrosion on titanium alloys that resembles crevice corrosion except that initiation may occur in the absence of normal crevices [SCH87].

Cathodic depolarizers, such as dissolved oxidizing species and H^+ ions, dramatically stimulate crevice corrosion initiation and propagation. The critical pH value at which crevice attack occurs varies among the commercial titanium alloys. In hot NaCl-based brines, critical pH levels can vary between 0.7 and 10.5 (Table 9.1), with the best resistance to crevice corrosion shown by the Ti-Pd alloys.

Table 9.1. Critical pH values for crevice corrosion of titanium alloys in hot ($\geq 90^\circ C$) NaCl brines [SCH87].

Alloy	Maximum pH at which attack occurs
Ti-6Al-4V	10-10.5
C.P. Titanium / Ti-3Al-2.5V	9.5-10
Ti-0.3 Mo - 0.8 Mo (Ti Gr 12)	2.5
Ti - 6 Al - 2 Sn - 4 Zr - 4 Mo	2
Ti - 3 Al - 8 V - 6 Cr - 4 Zr - 4 Mo	1
Ti - (0.04-0.25)Pd	0.7-0.8

Other cathodic depolarizing species such as dissolved oxygen, Fe^{+3} , Cu^{+2} , Ni^{+2} , and Ti^{+4} (see Table 9.2 for a more complete list) also enhance titanium's susceptibility to crevice corrosion. (Note this is in contrast to general corrosion where these oxidizing species tend to inhibit corrosion.) Oxygen is an effective accelerator of crevice corrosion even at concentrations of the order of tenths of a ppm. Although oxygen may only carry 15 to 30 percent of the total crevice corrosion current, it is essential for sustained crevice attack [IKE90]. Therefore deaerated solutions, devoid of any oxidizing species, will not cause significant crevice corrosion. A list of oxidizing anionic species which may diffuse into crevices and inhibit attack in halide-containing solutions is shown in Table 9.2.

Table 9.2. Dissolved oxidizing species which may accelerate or inhibit crevice corrosion of titanium in hot halide solutions [SCH87].

Accelerate Attack	Inhibit Attack
Fe^{+3} , Cu^{+2} , Ni^{+2} , Ti^{+4} , Ce^{+4} , Sn^{+4} , VO_2^+ , $\text{Te}^{+4,6}$, $\text{Se}^{+4,6}$, Hg^{+4} , $\text{Pt}^{+2,4}$, Pd^{+2} , Ru^{+3} , Ir^{+3} , Rh^{+3} , Au^{+3} , O_2 , Cl_2	OCl^- , ClO_3^- , ClO_4^{-2} , NO_3^- , $\text{Cr}_2\text{O}_7^{-2}$, MoO_4^{-2} , MnO_4^{-2} , $\text{S}_2\text{O}_3^{-2}$, VO_4^{-3} , VO_3^- , IO_3^- , WO_4^-

9.4 Physical characteristic of a susceptible crevice

Initiation of crevice corrosion on titanium alloys requires tight, deep crevices. Although the required physical dimensions do vary, typical conditions for aggressive attack are a crevice gap (or width) less than 15 μm and a crevice depth greater than 1 cm. Extremely tight (less than 0.5 μm) crevices (usually formed with sealants and gaskets against metal surfaces) result in greater susceptibility to attack under less aggressive pH/temperature conditions.

Titanium metal-to-metal crevices are generally much less susceptible to attack than gasket-to-metal crevices due to their inherently larger crevice gaps (typically greater than 10 μm).

Crevices created between two dissimilar titanium alloys have the crevice corrosion resistance of the more noble alloy because of the galvanically induced anodic protection. In addition, crevices formed between titanium and a number of dissimilar metals may also resist crevice corrosion while for other metals no such protection results (Table 9.3).

Table 9.3. Influence of dissimilar metal crevice members on the crevice corrosion resistance of CP titanium in hot chloride brines [SCH92a].

Inhibit attack	No inhibition
Precious metals (Pt, Pd, Ru, Ir, Rh)	Aluminum alloys
Copper alloys (brass and bronzes)	Zinc
Cu-Ni alloys	Silver
Ni alloys (Monel, 625, C-276)	Niobium
Ni-stainless steels (304, 316)	Molybdenum
Magnesium	Tin
Gold*	Lead

* not effective in hot Cl₂ saturated brines

Severe crevice corrosion may also occur under adherent deposits or scales on titanium metal surfaces [SCH92a]. Chloride, sulfate, and siliceous scales can support acidic-reducing conditions (favorable for crevice corrosion) within deposit-metal scales. In contrast, alkaline salt deposits such as carbonates will not support crevice attack. Scales containing significant amounts of oxidizing compounds, such as iron oxides, also inhibit crevice corrosion by passivating creviced metal surfaces.

9.5 Alloy Composition

Titanium alloys that are resistant to corrosion in hot reducing acids are also resistant to crevice corrosion attack. Alloying additions (≥ 0.04 wt.%) of platinum-group metal (Pt, Pd, Ru, and Ir) to practically any titanium alloy significantly enhance crevice corrosion resistance [SCH92a]. Alloys with Pd additions include titanium grades 7, 11, 16, 17, and 18. Nickel additions greater than 0.5 wt.% (as in Ti Gr 12) also increase titanium's crevice corrosion resistance to higher temperatures and lower pHs, relative to unalloyed titanium. Table 9.4 [SCH92a] and Figure 9.1 show that the crevice corrosion resistance of Ti Gr 7, 12, 16, and 18 is enhanced relative to unalloyed titanium.

Itoh et al [ITO89] demonstrated the superior crevice corrosion resistance of Ti Gr 7 and Gr 12 relative to C.P. titanium (Ti Gr 3). Testing was conducted in boiling 20% NaCl and crevices were formed with a Teflon grooved ring. Ti Gr 3 was susceptible to crevice corrosion at pH 6

Hydrogen embrittlement of titanium alloys is of concern when the long-term integrity of titanium is a consideration [BRA80]. The susceptibility of all the α -Ti alloys to hydrogen embrittlement is a concern [MCK85]. Although α -Ti alloys might be expected to suffer from embrittlement by hydrogen when gaseously charged (at high temperatures) to high hydrogen levels [WIL62], the examination of titanium tubes removed from a steam condenser after more than 10 years of operation with an impressed current for cathodic protection suggests that titanium is very resistant to this form of deterioration under normal operating conditions, even in polluted sea water [COV76b].

The discussion of the participation of hydrogen in stress corrosion cracking (SCC) will be presented in Section 12.0. The present section is limited to a discussion of bulk hydride formation. However, some information presented may be useful in understanding hydrogen involvement in SCC.

11.1 Mechanism

Two types of hydrogen embrittlement have been proposed [WIL62]: impact embrittlement and low-strain-rate embrittlement. Impact embrittlement due to hydrogen is observed in the α -Ti alloys. The loss of ductility results from the presence of a brittle hydride phase in the alloy. Impact embrittlement becomes more severe with increased hydrogen content, increased strain rate, decreased temperature, and the presence of notches. At room temperature severe embrittlement can result from as little as 150 ppm hydrogen in notched specimens of unalloyed titanium. The α -Ti alloys are the most susceptible to impact embrittlement, but sufficient hydrogen content can result in impact embrittlement of β - and α / β - Ti alloys.

Low-strain-rate embrittlement by hydrogen has been reported most often in α / β Ti alloys, but α -Ti alloys and β -Ti alloys are also vulnerable [WIL62]. Susceptibility increases with increasing hydrogen content and decreasing strain rate. A region of maximum susceptibility exists near room temperature, with the region becoming broader with increasing hydrogen content. It should be noted that there is no low-strain-rate embrittlement at high strain rates, which distinguishes it from impact embrittlement.

Both types of embrittlement are thought to result from a decrease in solubility of hydrogen in titanium alloys with decreasing temperature [WIL62]. The difference in behavior between the type of embrittlement is related to differences in the kinetics of titanium hydride precipitation.

11.2 Physical Properties

In α -Ti and α -Ti alloys the solubility of hydrogen is low; being about 20-200 ppm at room temperature [PAT74]. Dilation of the α titanium lattice by absorbed hydrogen has been determined by x-ray lattice spacing measurement. At higher hydrogen concentrations, titanium hydride formation occurs. The hydride, or δ phase, is a stable ordered compound with composition range $TiH_{1.53}$ to $TiH_{1.99}$. The regions of α and δ phases stability are shown in the titanium-hydrogen phase diagram (Fig. 11.1) [MAS90]. Note the increase in hydrogen solubility with increasing temperature. Determination of the hydrogen solubility in titanium is difficult because it is dependent on hydrogen pressure, stress, alloy composition, purity, and deformation [PAT74].

Titanium hydride has a CaF_2 crystal structure which consists of a face centered cubic arrangement of Ti ions with the hydrogen atoms located at the tetrahedral interstices. The lattice parameter of the fcc hydride phase is such that it has about 23 percent greater specific volume than α titanium. This large misfit results in non-coherent plate-shaped hydrides. A number of habit planes have been reported for titanium hydrides all of which correspond to possible slip or twinning planes in the alpha titanium lattice.

In β titanium, hydrogen solubility is considerably larger than it is in α titanium [PAT74]. For instance, more than 4000 ppm hydrogen are soluble in Ti-18Mo at room temperature. The body centered cubic lattice of the Ti-18Mo is expanded by 15% with the addition of 9000 ppm of hydrogen. Hydride formation in β -Ti alloys is not seen because at hydrogen concentrations above 10^4 ppm catastrophic failure occurs without the precipitation of hydrides.

Hydrogen diffusivity in α titanium is of the order of 10^{-10} to 10^{-11} cm^2/sec at $50^\circ C$. In the temperature range $25-100^\circ C$ the diffusivity of hydrogen in α titanium has been reported to be [PAT74]:

$$D = 6 \times 10^{-2} \exp(-14,400 \pm 800 \text{ cal} / RT) \text{ cm}^2 / \text{s}.$$

A determination of the diffusivity in the temperature range $610 - 900^\circ C$ gives a similar expression [PAP68]:

$$D = 3.0 \times 10^{-2} \exp(-14,700 \pm 650 \text{ cal / RT}) \text{ cm}^2 / \text{s}.$$

A slightly different expression for the diffusivity which was determined in the temperature range 500 - 824°C is given by [WAS54]:

$$D = 1.8 \times 10^{-2} \exp(-12,350 \text{ cal} \pm \text{cal / RT}) \text{ cm}^2 / \text{s}.$$

11.3 Effect of the Surface Layer on Hydrogen Uptake

The surface layer present on titanium greatly influences the rate of hydrogen uptake by titanium [TOM82]. The oxide layer provides a barrier to hydrogen uptake. For cathodic charging at low currents (2000 A/m²) polished specimens which were exposed to air prior to charging had a greater resistance to hydrogen uptake than those which were not exposed to air prior to charging. However this difference decreased with time and with increasing current density. This was due to the destruction of the protective oxide layer that formed upon exposure to air.

Surface preparation prior to oxidation also significantly influences the rate of hydrogen uptake [TOM82]. Etching of previous polished specimens prior to oxidation decreases the amount of hydrogen uptake by a factor of 10 at a charging current of 3000 Amps / m² after 5 hrs.

11.4 Effect of pH on Hydrogen Uptake

During cathodic polarization of α titanium at charging currents of 1.0 mA / cm², hydrogen absorption significantly decreases with increasing pH [PAT74]. For solutions of pH 0.3 and 1.3, the initial linear absorption rate becomes parabolic with increasing charging time. For solutions of pH 3.0, 4.6, and 7.3, decreasing linear rates of absorption were observed with increasing pH. For solutions of pH 10.3 and 14.0, no hydrogen absorption was detected. Similar results have been reported at higher charging currents (100 mA / cm²) [TOM82].

The rate-determining step in the hydrogen evolution reaction is believed to be electrochemical desorption [THO70]. Therefore, the number of adsorbed hydrogen atoms is expected to decrease with increasing pH producing a decrease of the amount of hydrogen absorbed. The minute amounts of hydrogen absorbed during charging in solutions of high pH may be explained by the stability of the oxide film [PAT74]. In the higher pH region a stable oxide film is expected to be

present on titanium. This oxide film may act as a barrier to hydrogen absorption. In addition, there is a change in the discharge step of the hydrogen evolution reaction as pH increases. It changes from $\text{H}_3\text{O}^+ + \text{e}^- = \text{H}_{\text{ads}} + \text{H}_2\text{O}$ to $\text{H}_2\text{O} + \text{e}^- = \text{H}_{\text{ads}} + \text{OH}^-$. This may affect the surface coverage of hydrogen atoms and thus the kinetics of hydrogen absorption.

11.5 Galvanic Coupling

In addition to gaseous hydrogen charging and electrochemical (cathodic) hydrogen charging, hydrogen absorption by titanium can be caused by galvanic coupling of titanium to a less noble material. Titanium galvanically coupled to aluminum in several aqueous electrolytes absorbs hydrogen, with the formation of surface hydrides [CHA68]. The electrolytes in the aqueous solutions were H_2SO_4 (pH 3.1), NH_4OH (pH 9.7), and 3.4 wt.% NaCl (pH 6.7). Hydrogen absorption occurred most readily in the acid solution. Surface preparation also significantly affected hydrogen uptake. Vapor blasted specimens offered the least resistance to hydrogen absorption, while etched specimens offered the most resistance.

Stressed specimens (U-bends) of titanium did not fail when galvanically coupled to aluminum in acid, basic, and salt solutions for 93 days [CHA68]. The stressed regions of the specimens absorbed more hydrogen than the unstressed regions. The hydride platelets which formed in the stressed region of the U-bends were oriented perpendicular to the tensile stress axis in the tension side, and they were oriented parallel to the stress axis in the compression side. This mode of precipitation is favored because the hydride is less dense than titanium.

A comprehensive study of cracking of both Ti Gr 2 and Gr 12 has been conducted by Clarke et al. [CLA86]. Using slow strain rate tests it was observed that the resistance to crack propagation of both grades is excellent in 3.5 % NaCl solution. However, the resistance of Ti Gr 12 breaks down under appropriate combinations of temperature and cathodic polarization. High cathodic polarization (to potentials below about -730mv (SHE)) and temperatures above 150°C are necessary to induce hydride cracking in Ti Gr 12. At most pH values, the free corrosion potential of titanium is well above the potential for hydrogen evolution and, hence, hydriding would not normally be expected to occur without a significant amount of cathodic polarization, unless the conditions become highly acidic or basic.

The decisive factor for the occurrence of hydrogen embrittlement at lower temperatures is whether or not hydrogen is taken up by the metal. This will depend not only upon the generation

13.0 Galvanic Corrosion

Titanium, provided it is in its normal passive state, is usually the cathode when galvanically coupled to most commercial structural alloys in service, that is, its corrosion potential is noble relative to most other alloys. For instance, the galvanic series in flowing sea water is shown in Table 13.1. Note that titanium's electrode potential is similar to or less noble than passive stainless steel and some nickel-base alloys (e.g. Alloy C and Monel 400). Alloy C is an early version of Alloy C-276. (Note Alloy C-22 is similar to Alloy C-276 under many conditions [GDO91], however, it does have a higher Cr content which may give it a different electrode potential.) Roy [ROY97] has determined that in several deaerated sodium chloride brine solutions ($2.5 < \text{pH} < 10.5$) Ti Gr 12 is less noble than Alloy C-22 by nominally 0.15 V. It should be noted that a material's position in a galvanic series is dependent on many variables. The composition of the solutions being one of the most important. Because of these small potential differences between titanium and these alloys negligible galvanic interactions might be expected provided passive conditions exist.

Table 13.1. Galvanic series in sea water flowing at 4 m/sec at 24°C [COT57].

Material	Steady State Electrode Potential (Volts vs. Saturated Calomel Electrode)
Graphite	0.25
Platinum	0.15
Zirconium	-0.04
316 Stainless Steel (passive)	-0.05
304 Stainless Steel (passive)	-0.08
Monel 400 (70Ni-30Cu)	-0.08
Alloy C	-0.08
Titanium	-0.10
Silver	-0.13
410 Stainless Steel (passive)	-0.15
316 Stainless Steel (active)	-0.18
Nickel	-0.20
430 Stainless Steel (passive)	-0.22
CDA 715 (70Cu-30Ni)	-0.25
CDA 706 (90Cu-10Ni)	-0.28
CDA 442 (admiralty brass)	-0.29
G Bronze	-0.31
CDA 687 (aluminum brass)	-0.32
Copper	-0.36
Alloy 464 (naval rolled brass)	-0.40
410 Stainless Steel (active)	-0.52
304 Stainless Steel (active)	-0.53
430 Stainless Steel (active)	-0.57
Carbon steel	-0.61
Cast iron	-0.61
Aluminum 3003-H	-0.79
Zinc	-1.03

When titanium is galvanically coupled to a more active metal, anodic attack of the active metal occurs and hydrogen charging of titanium may occur. The rates of the reactions depend on several factors, including the relative cathode to anode areas, temperature, concentration of cathodic depolarizer (e.g. O_2 and H^+), solution flow velocity, and solution chemistry [SCH86].

Under appropriate conditions, active metals may include carbon steels, aluminum, zinc, copper alloys, or stainless steels which are active or pitting. In ambient sea water the corrosion rates of various copper alloys can be accelerated by up to factors of 5-10 when coupled to titanium (Fig. 13.1). In addition high aqueous flow rates tend to accelerate galvanic copper alloy corrosion [SCH86].

Gases such as Cl_2 , Br_2 , and O_2 may also be produced in measurable amounts. If the gas-vapor phase contains N_2 , H_2 , CO_2 , Br_2 , Cl_2 , and O_2 , then irradiation may produce some HCl , HBr , HNO_3 , CO , O_3 , NH_3 , and various nitrogen oxides as products. The formation of these species is dependent on many factors including temperature, radiation dose rate, the amount of water present, and the ease of removal of the gases from solution.

Titanium alloys, in general, tend to perform well in oxidizing environments. Radiation tends to increase the number of oxidizing species in an environment. Corrosion testing of titanium under irradiation should, however, be investigated.

15.0 Additional Corrosion Studies of Titanium

Smailos et al. [SMA87] studied the corrosion susceptibility of Ti-0.2%Pd and Alloy C-4 (a Ni-Cr-Mo alloy) in deaerated salt solutions at temperatures up to 170°C and durations of up to 500 days (Table 15.1). Under none of the test conditions was Ti-0.2%Pd susceptible to crevice corrosion. However, Alloy C-4 was susceptible to crevice corrosion under certain conditions. General corrosion rates of both alloys were comparable.

Gegner and Wilson [GEG59] compared the corrosion resistance of unalloyed titanium with unalloyed zirconium, Monel, and Alloy C-276 in various chloride salt solutions (Table 15.2). In each case titanium had better corrosion resistance than the other materials tested.

The corrosion performance of Ti Gr 7 and 12 in various environments not covered elsewhere in this report is given in Appendix A. The corrosion performance of commercial purity Ti in various environments not covered elsewhere in this report is given in Appendix B.

Table 15.1. Crevice and general corrosion of Ti-0.2%Pd and Alloy C-4 in a deaerated brine solution [SMA87].

Material	Crevice Type	Surface Condition	Temperature / Time	Maximum Crevice Corrosion Depth (μm)	Radiation
Ti - 0.2%Pd	Metal/PTFE	As received	90°C / 582 d	no attack	No
	Metal/Metal	As received	90°C / 489 d 170°C / 286 d	no attack no attack	No No
	Metal/Metal	Polished	90°C / 266 d 170°C / 266 d	no attack no attack	No No
Alloy C-4	Metal/PTFE	As received	90°C / 582 d	250	No
	Metal/Metal	As received	90°C / 489 d 170°C / 286 d	70 non-uniform corrosion; black corrosion product	No No
	Metal/Metal	Polished	90°C / 266 d 170°C / 266 d	20 -	No No

Material	Temperature ($^{\circ}\text{C}$)	Exposure time (d)	Weight loss (g/m)	Corrosion rate ($\mu\text{m/a}$)
Ti-0.2%Pd	90	559	1.2 \pm 0.07	0.17 \pm 0.03
	170	529	0.46 \pm 0.07	0.07 \pm 0.03
	200	540	0.97 \pm 0.07	0.14 \pm 0.03
Alloy C-4	90	559	0.26 \pm 0.07	0.02 \pm 0.02
	170	368	1.48 \pm 0.07	0.17 \pm 0.02
	200	540	2.69 \pm 0.07	0.21 \pm 0.02

Table 15.2. Exposures of various metals to salt solutions [GEG59].

Environment	Temp (°C)	Duration (days)	Ti	Zr	Monel	Alloy C
Sea water sat'd w/ CO	24	160	0.003	0.01	4	--
Sea water; very high velocity	24	212	nil	0.05	172,5	--
Sat'd NaCl brine; pH 10.4	57	125	nil	0.001	0.08 ⁶	nil
Sat'd NaCl Brine	21	208	nil	0.004	0.6 ⁶	nil
Sat'd NaCl Brine	60	169	0.0006	0.007	0.05 ⁶	0.002 ⁶
Sat'd KCl Brine	60	183	0.0002	0.009	0.02 ⁶	0.002
Sat'd NaCl brine	71	163	nil	0.01	0.04 ⁶	0.02
20% NaCl brine; pH 2.0-4.5	74	73	0.01	19 ^{5,8}	>90 ¹	12; 0.1 ⁹

- 1) Specimens were completely consumed during the test.
- 2) One of two duplicate specimens was lost.
- 3) Shallow or slight pitting attack.
- 4) Moderate pitting attack.
- 5) Severe pitting attack.
- 6) Slight attack under spacer.
- 7) Moderate attack under spacer.
- 8) Sever attack under spacer.
- 9) One of two specimens suffered severe pitting and under-spacer attack.

16.0 CONCLUSIONS

Of the materials reviewed, commercially pure titanium, Ti Gr 2, is the most susceptible to crevice corrosion. Ti Gr 7, 12, and 16 are likely to be very resistant to crevice corrosion under the current expected Yucca Mountain repository conditions. Although Grade 7 has the greatest resistance to crevice corrosion it is also the most expensive.

Although the possibility of SLC exists, it has not yet been observed in α Ti alloys. For hydride precipitation to occur at temperatures in excess of 100°C, the hydrogen concentration would need to be relatively high, much higher than the maximum amount of hydrogen allowed during the manufacture of α Ti alloys (0.015 wt%).

A large amount of SCC data accumulated at SNL and BNL for the WIPP program and by the Canadian Waste Management Program on titanium grades 2 and 12 indicates that there is no SCC at naturally occurring potentials in various brines.

Hydride induced cracking of titanium is a possibility and, therefore, further investigation of this phenomenon under credible repository conditions is warranted.

One disadvantage of titanium and its alloys is that their strengths decrease rather rapidly with increasing temperature. This is due to the strong temperature dependence of interstitial solute strengthening mechanisms.

Ti Gr 7, 12 and 16 are recommended for further consideration as candidate materials for high level nuclear waste packages due to their very good corrosion resistance under plausible repository conditions.

17.0 Acknowledgments

Work performed under the auspices of the U.S. Department of Energy by Lawrence Livermore National Laboratory under Contract W-7405-ENG-48. This work is supported by Yucca Mountain Site Characterization Project, LLNL.

The author wishes to thank Hira S. Ahluwalia for his initial compilation of the relevant literature.

18.0 REFERENCES

- ABR81 L. Abrego and H.L. Rack, "The Slow Strain Rate Behaviour of TiCode 12 (ASTM Gr.12) in Aqueous Chloride Solutions", CORROSION/81, NACE, Houston Texas, 1981.
- AHN82 T.M. Ahn and P. Soo, "Container Assessment-Corrosion Study of HLW Container Materials, Quarterly Progress Report, Oct-Dec 1981," NUREG/Cr-2317, BNL-NUREG-51499, i (4), Brookhaven National Laboratory (April 1982)
- AND64 V.V. Andreeva, "Behavior and Nature of Thin Oxide Films on Some Metals in Gaseous Media and in Electrolyte Solutions," Corrosion, Vol. 20, 1964, pp. 35t-46t.
- ASTM ASTM Designation: B 265 - 95a "Standard Specification for Titanium and Titanium Alloy Strip, Sheet, and Plate," American Society for Testing and Materials, Philadelphia, PA, 1997.
- BOM54 H.B. Bomberger, P.J. Cambourelis, and G.E. Hutchinson, "Corrosion Properties of Titanium in Marine Environments," J. of the Electrochemical Society, Vol. 101, 1954, p. 442.
- BOY78 R.R. Boyer and W.F. Spurr, "Characteristics of Sustained-Load Cracking and Hydrogen Effects in Ti-6Al-4V", Metallurgical Transactions A, Vol. 9A, 1978, pp. 23-29.
- BOY85 R.R. Boyer, "Titanium and Titanium Alloys," in Metals Handbook 9th Edition, Vol. 9, Metallography and Microstructures, American Society for Metals, Metals Park, Ohio, 1985, pp. 458-475.
- BRA80 J.W. Braithwaite and M.A. Molecke, "Nuclear Waste Canister Corrosion Studies Pertinent to Geologic Isolation," Nuclear and Chemical Waste Management, Vol. 1, 1980, pp. 37-50.
- BRA80b J.W. Braithwaite, N.J. Magnami, and J.W. Munford, "Titanium Alloy Corrosion in Nuclear Waste Environments," Sandia Laboratories CONF-800305--5, 1980.
- CHA68 L.A. Charlot and R.E. Westerman, "Low-Temperature Hydriding of Zircaloy-2 and Titanium in Aqueous Solutions," Electrochemical Technology, Vol. 6, No. 3-4, 1968, pp. 132-137.
- CLA86 C.F. Clarke, D. Hardie, and P. McKay, "The Cracking of Titanium in Hot Aqueous Sodium Chloride Solutions", Corrosion Science, Vol. 26, No. 6, 1986, pp. 425-440.
- COT57 J.B. Cotton and B.P. Dowing, "Corrosion Resistance of Titanium to Seawater," Trans. Inst. Marine Engineering, Vol. 69, No. 8, 1957, pp. 311.
- COV76 L.C. Covington, "Pitting Corrosion of Titanium Tubes in Hot Concentrated Brine Solutions," Galvanic and Pitting Corrosion-Field and Laboratory Studies, ASTM STP 576, ASTM, Philadelphia, Pennsylvania, 1976, p. 147

- COV76b L.C. Covington, W.M. Parris, and D.M. McCue, CORROSION/76, Paper 79, NACE, Houston, Texas, 1976.
- COV77 L.C. Covington, "Titanium Solves Corrosion Problems in Petroleum Processing," Metal Progress, Vol. 111, No. 2 (Feb 1977) pp. 38-45.
- COV79 L.C. Covington, "The Influence of Surface Condition and Environment on the Hydriding of Titanium," Corrosion, Vol 35, No. 8, 1979, pp. 378-382.
- COV89 L.C. Covington and P.A. Schweitzer, "Titanium," in Corrosion and Corrosion Protection Handbook, Second Edition, P.A. Schweitzer, ed., Marcel Dekker, Inc., New York, 1989, Chap. 10.
- CRA95 B.D. Craig and D.S. Anderson, eds., Handbook of Corrosion Data, ASM International, Materials Park, OH 44073, 1995, pp. 55-61.
- CUR69 R.E. Curtis, R.R. Boyer, and J.C. Williams, "Relationship Between Composition, Microstructure, and Stress Corrosion Cracking (in Salt Solutions) in Titanium Alloys" Trans. ASM 62, 457, 1969.
- DON88 M.J. Donachie, **Titanium; A Technical Guide**, ASM International, Metal Park, Ohio, 1988.
- FEI70 N.G. Feige and R.L. Kane, "Experience with Titanium Structures in Marine Service," Materials Protection and Performance, Vol. 9, No. 8, Aug. 1970, pp. 13.
- GDO91 G.E. Gdowski, "Survey of Degradation Modes of Four Nickel-Chromium-Molybdenum Alloys," Lawrence Livermore National Laboratory Report UCRL-ID-108330, March 1991.
- GEG59 P.J. Gegner and W.L. Wilson, "Corrosion Resistance of Titanium and Zirconium in Chemical Plant Exposures," Corrosion, Vol. 15, No. 7, July 1959, pp. 341t-350t.
- GRI68 J.C. Griess, "Crevice Corrosion of Titanium in Aqueous Salt Solutions," Corrosion, Vol. 24, No. 4, April 1968, pp. 96-109.
- IKE90 B.M. Ikeda, et al., "The Effect of Temperature on Crevice Corrosion of Titanium," Proceedings of the 11th International Corrosion Congress, Vol. 5, Florence, Italy, April 1990.
- ITO89 H. Itoh, K. Kitaoka, Y. Tsumori, H. Satoh, and T. Furuya, "Crevice Corrosion Resistance and Mechanical Properties of ASTM Grade 12 Titanium Alloy," KOBELCO Technol. Rev., Vol. 6, 1989, pp. 41-45.
- KOI73 T. Koizumi and S. Furuya, "Pitting Corrosion of Titanium in High Temperature Halide Solutions," Proc. 2nd Int. Conf. Titanium Sci. Technol., Plenum, New York, 1973, pp. 2383-2393.

- LAM90 S. Lampman, "Wrought Titanium and Titanium Alloys," Metals Handbook, 10th Edition; Vol. 2, Properties and Selection: Nonferrous Alloys and Special-Purpose Materials, ASM International, 1990, pp. 592-633.
- LAN66 I.R. Lane, J.L. Cavallaro, and A.G.S. Morton, "Sea Water Embrittlement of Titanium", in Stress Corrosion Cracking of Titanium, ASTM STP 397, 246, 1966.
- LEE81 J.B. Lee, "Elevated Temperature Potential - pH Diagrams for the Cr-H₂O, Ti-H₂O, Mo-H₂O, and Pt-H₂O Systems," Corrosion, Vol. 37, No. 8, Aug. 1981, pp. 467-481.
- MAR76 H. Margolin, "Stress, hydrogen Segregation, and fracture in α - β Titanium Alloys," Metallurgical Transactions A, Vol. 7A, 1976, pp. 1233-1235.
- MAS90 T.B. Massalski, editor-in-chief, Binary Alloys Phase Diagrams; Second Edition, ASM International, 1990, pp. 2675-2679, 2874-2876, 3058-3060.
- MAT84 H. Mattsson and I. Olefjord, "General Corrosion of Ti in Hot Water and Water Saturated Bentonite Clay," SKB Technical Report 84-19, Swedish Nuclear Fuel and Waste Management Co., Stockholm, Dec. 1984.
- MAT85 H. Mattsson and I. Olefjord, "ESCA Investigation of the Reaction Products Formed on Titanium Exposed to Water Saturated Bentonite Clay," in Scientific Basis for Nuclear Waste Management IX, L.O. Werme, ed., Materials Research Society Symposium, Vol. 50, 1985, pp. 481-490.
- MCC96 R.D. McCright, Scientific Investigation Plan SIP-CM-1 Rev. 3, "Metal Barrier Selection and Testing," Lawrence Livermore National Laboratory Yucca Mountain Project, 1996.
- MCK84 P. McKay, "Crevice Corrosion of Ti - 0.8% Ni - 0.3% Mo Alloy (ASTM Grade-12 in Chloride Environments at Elevated Temperature," Proceedings of the 9th International Congress on Metallic Corrosion, June 1984, Vol. 3, National Research Council of Canada, Ottawa, Canada, pp. 288-297.
- MCK85 P. McKay and D.B. Mitton, "An Electrochemical Investigation of Localized Corrosion on Titanium in Chloride Environments", Corrosion, Vol. 41, No. 1, Jan. 1985, pp. 52-62.
- MEY74 D.A. Meyn, "Effect of Hydrogen on Fracture and Inert-Environment Sustained Load Cracking Resistance of α - β Titanium Alloys", Metallurgical Transactions, Vol. 5, Nov. 1974, pp. 2405-2414.
- MIN78 W.W. Minkler, "Titanium for Chemical Processing Equipment," Metal Progress, Vol. 113, No. 2 (Feb 1978), pp. 27-31.
- MOL83 M.A. Molecke, J.A. Rupen, and R.N. Diegle, "Materials for High-Level Waste Canister/Overpacks in Salt Formations," Nuclear Technology, Vol. 63, Dec. 1983, pp. 476-506.

- NUT81 K. Nuttall and V.F. Urbanic, "An Assessment of Materials for Nuclear Fuel Immobilization Containers", AECL-6440, Whiteshell Nuclear Research Establishment, Manitoba, September 1981.
- OET76 T.P. Oettinger and M.G. Fontana, "Austenitic Stainless Steel and Titanium for Wet Oxidation of Sewage Sludge," *Materials Performance*, Vol. 15, No. 11, Nov. 1976, pp. 29-35.
- OLD78 J.W. Oldfield and W.H. Sutton, "Crevice Corrosion of Stainless Steels; I. A Mathematical Model," *British Corrosion Journal*, Vol. 13, 1978, pp. 13-22.
- PAP68 T.P. Papazoglou and M.T. Hepworth, "The Diffusion of Hydrogen in Titanium," *Trans. of the Metallurgical Society of AIME*, Vol. 242, April 1968, pp. 682-685.
- PAT74 N.E. Paton and J.C. Williams, "Effect of Hydrogen on Titanium and Its Alloys," **Hydrogen in Metals**, I.M. Bernstein, A.W. Thompson, eds., American Society for Metals, 1974, pp. 409-432.
- PET80 J.A. Petit, G. Chatainier, P. Lafargue, and F. Dabosi, "Electrochemical Behaviour of Titanium-Nickel Alloys in Sulfuric Acid Media," in *Titanium 80*, Vol. 4, Science and Technology, Proceedings of the 4th International Conference on Titanium, Kyoto, Japan, May 19-22 (1980), The Metallurgical Society of AIME, pp. 2659-2667.
- ROY96 A.K. Roy, D.A. Jones, and R.D. McCright, "Degradation Mode Survey; Galvanic Corrosion of Candidate Metallic Materials for High-Level Radioactive Waste Disposal Containers," Lawrence Livermore National Laboratory Report UCRL-ID-125645, November 1996.
- ROY97 A.K. Roy, personal communication.
- RUP81 J.A. Ruppen, M.A. Molecke, R.S. Glass, "Titanium Utilization in Long-Term Nuclear Waste Storage," *Titanium for Energy and Industrial Applications*, TMS-AIME, 1981, pp. 355-369.
- SAN69 G. Sandoz, Proceedings of Conference on Fundamental Aspects Of Stress Corrosion, p689, NACE, Houston 1969.
- SCH56 D. Schlain and C.B. Kenahan, "The Role of Crevices in Decreasing the Passivity of Titanium in Certain Solutions", *Corrosion*, Vol. 12, No. 8, Aug. 1956, pp. 422t-426t.
- SCH81 R.W. Schutz and L.C. Covington, "Effect of Oxide Films on the Corrosion Resistance of Titanium," *Corrosion*, Vol 37, Oct. 1991, pp. 585-591.
- SCH85 R.W. Schultz, "Performance and Application of Titanium Alloys in Geothermal Brine Service," *Materials Performance*, Vol. 24, No. 1, 1985, pp. 39-47.
- SCH86 R.W. Schultz, "Titanium," *Process Industries Corrosion*, National Association of Corrosion Engineers, Houston, 1986, pp. 503-526.

- SCH87 R.W. Schutz and D.E. Thomas, "Corrosion of Titanium and Titanium Alloys," in **ASM Metals Handbook, 9th Edition, Vol. 13, Corrosion**, ASM International, Materials Park, Ohio, 1987, pp. 669-706.
- SCH92a R.W. Schutz, "Understanding and Preventing Crevice Corrosion of Titanium Alloys; Part I," *Materials Performance*, Oct. 1992, pp. 57-62.
- SCH92b R.W. Schutz, "Understanding and Preventing Crevice Corrosion of Titanium Alloys; Part II," *Materials Performance*, Nov. 1992, pp. 54-56.
- SCH93 R.W. Schutz and M. Xiao, "Optimized Lean-Pd Titanium Alloys for Aggressive Reducing Acid and Halide Service Environments," 12th International Corrosion Congress, Houston, TX, Sept. 1993, National Association of Corrosion Engineers.
- SED72 A.J. Sedriks, J.A.S. Green, and D.L. Novak, "Electrochemical Behavior of Ti-Ni Alloys in Acidic Chloride Solutions," *Corrosion*, Vol. 28, No. 4, April 1972, pp. 137-142.
- SHI78 K. Shimogori, H.Sato, and H.Tomari, "Crevice Corrosion of Titanium in NaCl Solutions in the Temperature Range 100 to 250°C," *J.of the Japan Institute of Metals*, Vol. 42, 1978, pp. 567-572.
- SOR85 N.R. Sorensen and J.A. Ruppen, "The Environmental Cracking of Ticode-12 in Aqueous Chloride Environments," *Corrosion*, Vol. 41, No. 10, Oct. 1985, pp. 560-569.
- SMA87 E. Smailos, W. Schwarzkopf, R. Koster, "Corrosion Behavior of Container Materials for the Disposal of High-Level Waste forms in Rock Salt Formations," Report # KfK 4265 (ISSN 0303-4003), May 1987.
- SMA81 R.E. Smallwood, ASTM STP728, American Society for Testing and Materials, 1981, pp. 147-162.
- THO70 N.T. Thomas and K. Nobe, "Kinetic of the Hydrogen Evolution Reaction on Titanium," *J. of the Electrochemical Society*, Vol. 117, No. 5, May 1970, pp. 622-626.
- TOM82 N.D. Tomashov, G.P. Chernova, V.I. Kasarin, E.G. Mansky, T.A. Fedoseeva, V.V. Krasnoyarsky, and T.P. Stepanova, "Corrosion and Passivity of The Cathode-Modified Titanium-Based Alloys," *Titanium and Titanium Alloys - Scientific and Technological Aspects*, Vol. 2, J.C. Williams, A.F. Belov, eds., Plenum Press, New York, 1982, pp. 915-925.
- WAS54 R.J. Wasilweski and G.L. Kehl, "Diffusion of Hydrogen in Titanium," *Metallurgica*, Vol. 50, Nov. 1954, pp. 225-230.
- WIL74 D.N. Williams, "Subcritical Crack Growth Under Sustained Load", *Metallurgical Transactions*, Vol. 5, 1974, pp. 2351-2358.
- WIL76 D.N. Williams, "Effects of Hydrogen in Titanium Alloys on Subcritical Crack Growth Under Sustained Load", *Materials Science and Engineering*, Vol. 24, 1976, pp. 53-63.

WIL62

D.N. Williams, "The Hydrogen Embrittlement of Titanium Alloys," J. of the Institute of Metals, Vol. 91, 1962-63, pp. 147-152.

Appendix A. Corrosion Data for Titanium Alloys Grade 7 and 12 [GRA95]. Data is a compilation from numerous published sources [GRA95]. Data does not indicate if other forms of corrosion such as localized corrosion had occurred. Duration of testing is not stated. Bold entries indicate species that are components of the naturally occurring waters at Yucca Mountain.

Medium	Alloy	Concentration (%)	Temperature (°C)	Corrosion Rate (mm/yr)
Acetic acid + 5% formic acid	Gr 12	58	Boiling	nil
Ammonium hydroxide	Gr 12	30	Boiling	nil
Aluminum chloride	Gr 12	10	Boiling	nil
	Gr 7	10	100	<0.025
	Gr 7	25	100	0.025
Ammonium chloride	Gr 12	10	boiling	nil
Aqua regia	Gr 7	3:1	Boiling	1.12
	Gr 12	3:1	Boiling	0.61
Calcium chloride	Gr 7	62	150	nil
	Gr 7	73	177	nil
Chlorine, wet	Gr 7	---	25	nil
Chromic acid	Gr 7	10	Boiling	nil
Citric acid	Gr 7	50	Boiling	0.025
	Gr 12	50	Boiling	0.013
Ferric chloride	Gr 7	10	Boiling	nil
	Gr 12	10	Boiling	nil
	Gr 7	30	Boiling	nil
Formic acid	Gr 7	45	Boiling	nil
	Gr 12	45, 50	Boiling	nil
	Gr 7	50	Boiling	0.01
	Gr 12	90	Boiling	0.56
	Gr 7	90	Boiling	0.056
Hydrochloric acid, deaerated	Gr 7	3	82	0.013
	Gr 7	5	82	0.051
	Gr 7	10	82	0.419

Hydrochloric acid	Gr 7	0.5	Boiling	nil
	Gr 7	1.0	Boiling	0.008
	Gr 7	1.5	Boiling	0.03
	Gr 7	5.0	Boiling	0.23
	Gr 12	0.5	Boiling	nil
	Gr 12	1.0	Boiling	0.04
	Gr 12	1.5	Boiling	0.25
Hydrochloric acid, hydrogen saturated	Gr 7	1-15	25	<0.025
	Gr 7	20	25	0.102
	Gr 7	5	70	0.076
	Gr 7	10	70	0.178
	Gr 7	15	70	0.33
	Gr 7	3	190	0.025
	Gr 7	5	190	0.102
	Gr 7	10	190	8.9
Hydrochloric acid, oxygen saturated	Gr 7	3, 5	190	0.127
	Gr 7	10	190	9.3
Hydrochloric acid, chlorine saturated	Gr 7	3,5	190	<0.03
	Gr 7	10	190	29.0
Hydrochloric acid, aerated	Gr 7	1, 5	70	<0.03
	Gr 7	10	70	0.05
	Gr 7	15	70	0.15
Hydrochloric acid + 4% FeCl ₃ + 4% MgCl ₂	Gr 7	19	82	0.49
Hydrochloric acid + 4% FeCl ₃ + 4% MgCl ₂ , chlorine saturated	Gr 7	19	82	0.46
Hydrochloric acid + 5 g/l FeCl ₃ + 16 g/l FeCl ₃ + 16 g/l CuCl ₂	Gr 7	10	Boiling	0.279
	Gr 7	10	Boiling	0.076
	Gr 7	10	Boiling	0.127
Hydrochloric acid + 2 g/l FeCl ₃ + 0.1% FeCl ₃ + 0.1% FeCl ₃	Gr 12	4.2	91	0.058
	Gr 7	5	Boiling	0.013
	Gr 12	5	Boiling	0.020
Hydrochloric acid + 18% H ₃ PO ₄ + 5% HNO ₃	Gr 7	18	77	nil

Hydrogen peroxide				
pH 1	Gr 7	5	23	0.062
pH 4	Gr 7	5	23	0.010
pH 1	Gr 7	5	66	0.127
pH 4	Gr 7	5	66	0.046
+ 500 ppm Ca ²⁺ , pH 1	Gr 7	5	66	nil
+ 500 ppm Ca ²⁺ , pH 1	Gr 7	20	66	0.76
Hydrogen peroxide, pH 1 + 5% NaCl	Gr 7	20	66	0.008
Magnesium chloride	Gr 7	Saturated	Boiling	nil
Oxalic acid	Gr 7	1	Boiling	1.14
Phosphoric acid, naturally aerated	Gr 12	25	25	0.019
	Gr 12	30	25	0.056
	Gr 12	45	25	0.157
	Gr 12	8	52	0.02
	Gr 12	13	52	0.066
	Gr 12	15	52	0.52
	Gr 12	5	66	0.038
	Gr 12	7	66	0.15
	Gr 12	0.5	Boiling	0.071
	Gr 12	1.0	Boiling	0.14
	Gr 7	40	25	0.008
	Gr 7	60	25	0.07
	Gr 7	15	52	0.036
	Gr 7	23	52	0.15
	Gr 7	8	66	0.076
	Gr 7	15	66	0.104
	Gr 7	0.5	Boiling	0.050
	Gr 7	1.0	Boiling	0.107
	Gr 7	5.0	Boiling	0.228
Sodium fluoride	Gr 12	1	Boiling	0.001
pH 7	Gr 7	1	Boiling	0.002
Sodium sulfate, pH 1	Gr 7	10	Boiling	nil
Sulfamic acid	Gr 12	10	Boiling	11.6
	Gr 7	10	Boiling	0.37

Sulfuric acid, naturally aerated	Gr 12	9	24	0.003
	Gr 12	9.5	24	0.006
	Gr 12	10	24	0.38
	Gr 12	3.5	52	0.013
	Gr 12	3.75	52	1.73
	Gr 12	2.75	66	0.015
	Gr 12	3.0	66	1.65
	Gr 12	0.75	Boiling	0.003
	Gr 12	1.0	Boiling	0.91
	Gr 7	1.0	204	0.005
	Gr 7	2.0	204	nil
	Gr 12	1.0	204	0.91
Sulfuric acid, nitrogen saturated	Gr 7	5	70	0.15
	Gr 7	10	70	0.25
	Gr 7	1,5	190	0.13
	Gr 7	10	190	1.50
Sulfuric acid, oxygen saturated	Gr 7	1-10	190	0.13
Sulfuric acid, chlorine saturated	Gr 7	10	190	0.051
	Gr 7	20	190	0.38
Sulfuric acid, nitrogen saturated	Gr 7	10	25	0.025
	Gr 7	40	25	0.23
Sulfuric acid, aerated	Gr 7	10	70	0.10
	Gr 7	40	70	0.94
Sulfuric acid + 5 g/l $\text{Fe}_2(\text{SO}_4)_3$	Gr 7	10	Boiling	0.178
Sulfuric acid + 16 g/l $\text{Fe}_2(\text{SO}_4)_3$	Gr 7	10	Boiling	<0.03
Sulfuric acid + 16 g/l $\text{Fe}_2(\text{SO}_4)_3$	Gr 7	20	Boiling	0.15
Sulfuric acid + 15% CuSO_4	Gr 7	15	Boiling	0.64
Sulfuric acid + 1% CuSO_4	Gr 7	30	Boiling	1.75
Sulfuric acid + 100 ppm Cu^{2+} + 1% thiourea (deaerated)	Gr 7	1	100	nil
	Gr 12	1	100	0.23

Sulfuric acid + 1000 ppm Cl ⁻	Gr 7	15	49	0.015
---	------	----	----	-------

Appendix B. Corrosion Data for Unalloyed Titanium [GRA95]. Data is a compilation from numerous published sources [GRA95]. Data does not indicate if other forms of corrosion such as localized corrosion had occurred. Duration of testing is not stated. Entries are limited to corrosion of components of the naturally occurring components at Yucca Mountain and major elements of candidate materials.

Medium	Concentration (%)	Temperature (°C)	Corrosion Rate (mm/yr)
Calcium carbonate	saturated	boiling	nil
Calcium chloride	5	100	0.005
	10	100	0.007
	20	100	0.015
	55	104	0.001
	60	149	<0.003
	62	154	0.406
	73	175	0.80
Calcium hydroxide	saturated	room	nil
	saturated	boiling	nil
Copper nitrate	saturated	room	nil
Copper sulfate	50	boiling	nil
Copper sulfate + 2% H ₂ SO ₄	saturated	room	0.018
Cupric carbonated + cupric hydroxide	saturated	ambient	nil
Cupric chloride	20	boiling	nil
	40	boiling	0.005
	55	118	0.003
Cuprous chloride	50	90	<0.003
Ferric chloride	10-20	room	nil
	1-30	100	0.004
	10-40	boiling	nil
	1-30	boiling	nil
	50	150	0.003
Ferric chloride	10	boiling	0.00
Ferric sulfate	10	room	nil
Ferrous chloride + 0.5% HCl	30	79	0.006

Ferrous sulfate	saturated	room	nil
Fluorosilicic acid	10	room	47.5
Hydrofluoric	1	26	127
Hydrofluori-nitric acid 5 vol% HF - 35 vol% HNO ₃		25	452
		35	571
Magnesium chloride	5-20	100	<0.010
Magnesium hydroxide	saturated	room	nil
Magnesium sulfate	saturated	room	nil
Nickel chloride	5	100	0.004
	20	100	0.003
Nickel nitrate	50	room	nil
Potassium chloride	saturated	room	nil
	saturated	60	nil
Potassium hydroxide	50	29	0.010
	10	boiling	<0.127
	25	boiling	0.305
Potassium sulfate	10	room	nil
Seawater		24	nil
Seawater, 4.5 yr test		ambient	nil
Sodium carbonate	25	boiling	nil
Sodium chloride	saturated	room	nil
pH 7	23	boiling	nil
pH 1.5	23	boiling	nil
pH 1.2	23	boiling	0.71
pH 1.2; some dissolved chlorine	23	boiling	nil
Sodium fluoride	saturated	room	0.008
pH 7	1	boiling	0.001
pH 10	1	boiling	0.001
pH 7	1	204	0.000

Sodium nitrate	saturated	room	nil
Sodium silicate	25	boiling	nil
Sodium sulfate	10-20 saturated	boiling room	nil nil
Steam + air		82	nil

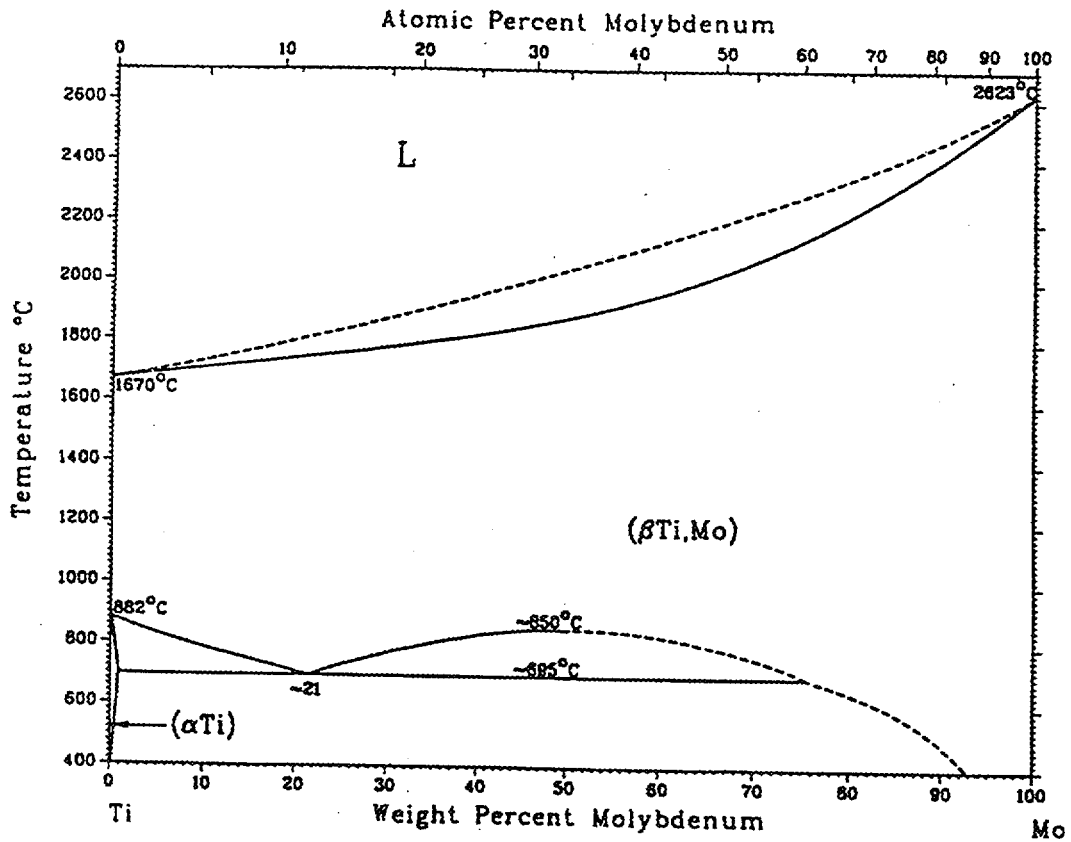
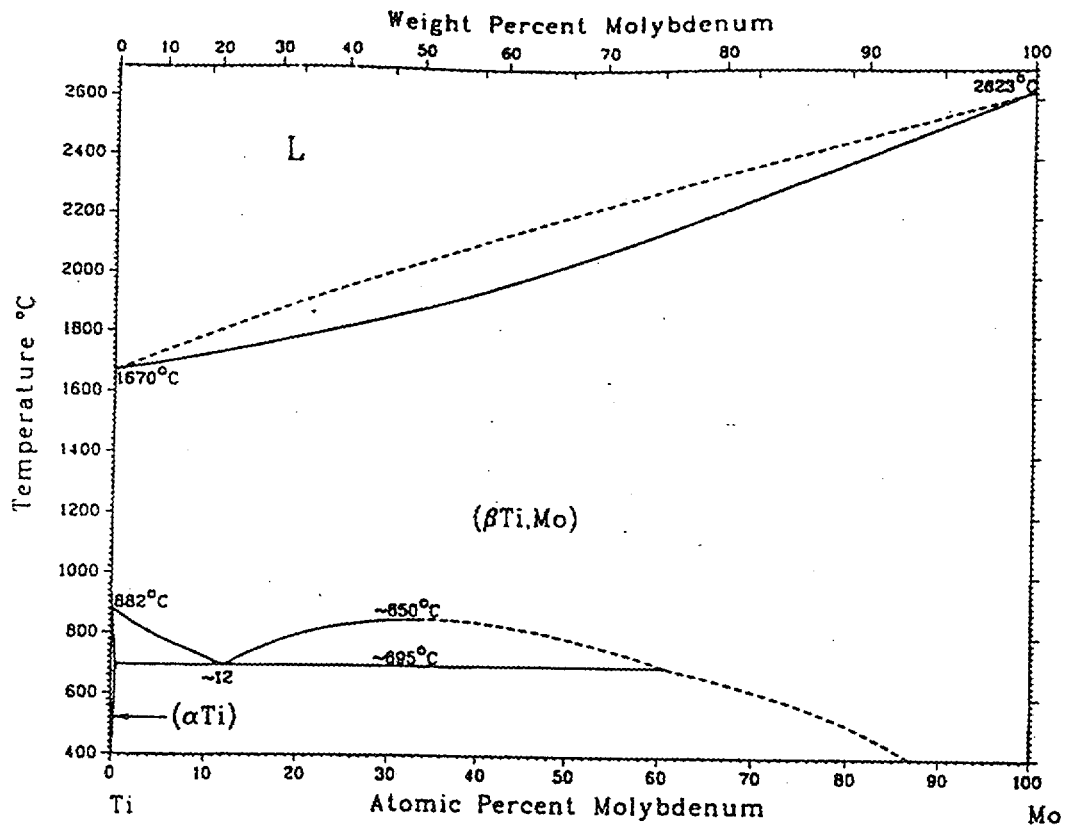


Fig. 2.3 Molybdenum-titanium phase diagram [MAS90].

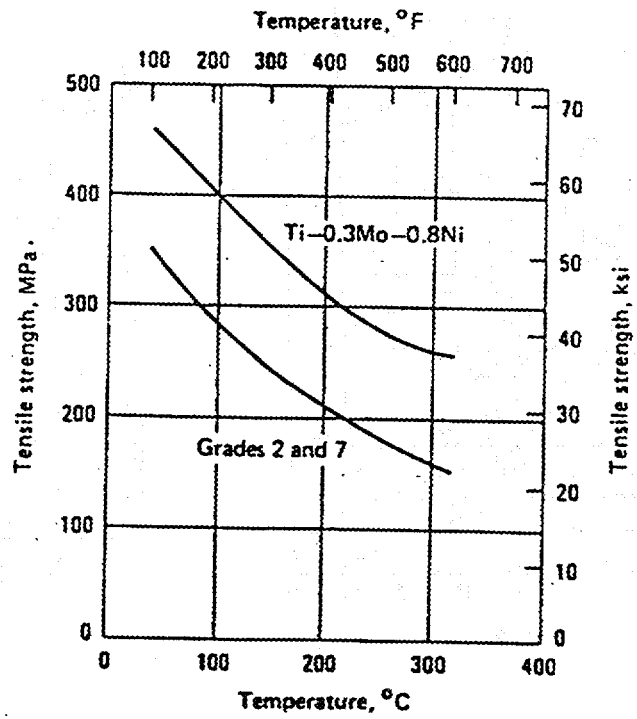


Fig. 3.1 Minimum tensile strength of low-strength titanium alloys [LAM90].

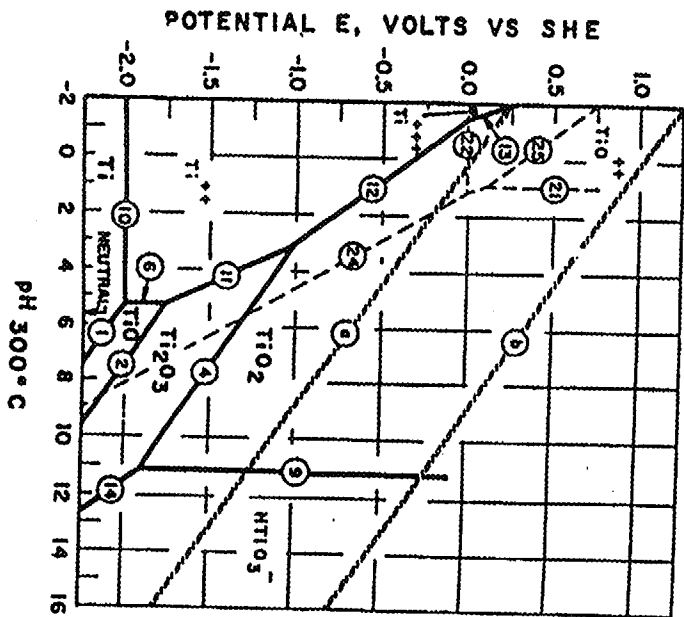
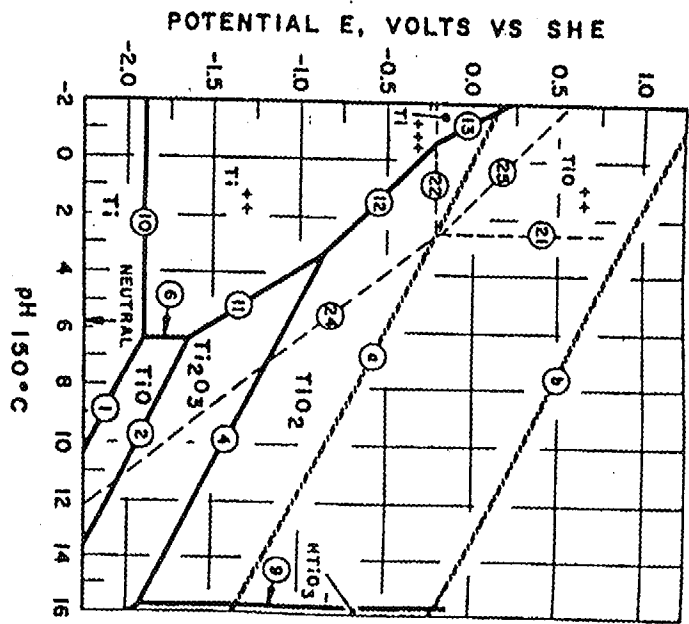
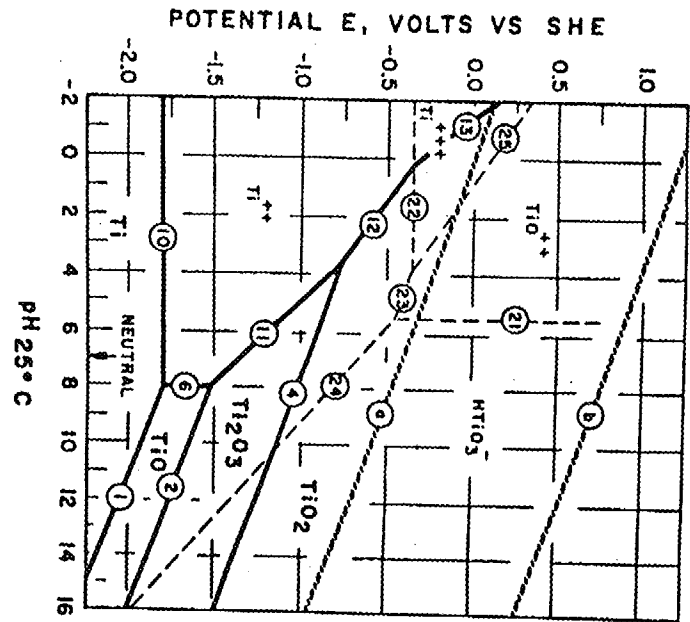


Fig. 6.1 Pourbaix diagrams for $Ti-H_2O$ at 25, 150, and 300°C [LEE81].

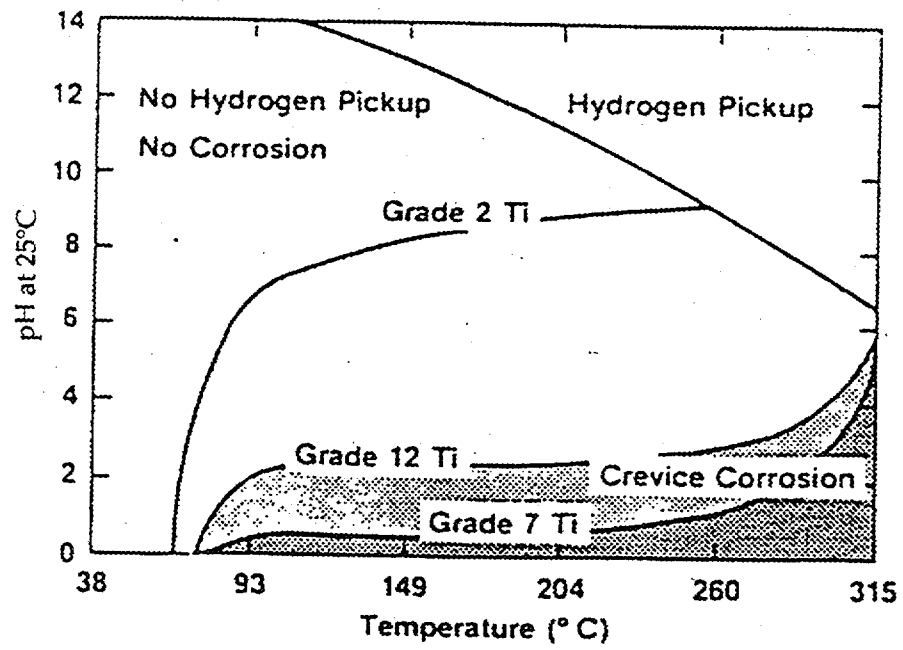


Fig. 9.1 Temperature - pH limits for crevice corrosion of titanium alloys in concentrated NaCl brines [SCH85]

